Waves of Extinction from Sterile Insect Release

M. A. LEWIS
Department of Mathematics, University of Utah, Salt Lake City, Utah 84112

AND

P. VAN DEN DRIESSCHE
*Department of Mathematics and Statistics, University of Victoria,
Victoria, B.C., V8W 3P4, Canada*

Received 29 July 1992; revised 13 November 1992

ABSTRACT

Employing theoretical models, we show that the sterile insect release method (SIRM) can give rise to traveling waves of fertile insects. The velocity of these waves depends critically upon the density of sterile insects (and thus upon the rate at which sterile individuals are being released into the environment). When the sterile density is sufficiently low, the traveling wave advances, giving rise to an invasion. However, when the sterile density exceeds a critical threshold, the wave reverses direction, thereby retreating and giving rise to local extinction. Both analytical (regular perturbation) methods and numerical methods are used to determine wave velocities and wave profiles. This is the first time traveling wave solutions have been shown for the SIRM.

---

1. INTRODUCTION

Release of sterile insect pests may be used to control the density of fertile pests, diluting their reproductive capacity, and eventually leading to a population "crash" and local extinction. Originally suggested by Knipling [15], this sterile insect release method (SIRM) has been applied successfully in field conditions against species such as the screwworm fly [5, 16], the fruit fly [14], the codling moth [28], and the pink bollworm [11].

Concurrent with the application of such biological control methods has been an explosion in the number of SIRM mathematical models (see, e.g., [1], [3], [4], [6]–[8], [13], [19], [21], [25]–[27]) as well as SIRM computer models (see, e.g., [20], [26]) for quantitatively assessing their effectiveness. However, with few exceptions, SIRM mathematical mod-

655 Avenue of the Americas, New York, NY 10010 0025-5564/93/$6.00

els have ignored the spatial aspects of controlling insect pests (but see [19], [25]).

Spatial considerations are significant for two reasons. First, any environment is likely to vary spatially, and thus key ecological parameters, such as intrinsic growth rates, carrying capacity, and mortality, are likely to differ between locations. The result may be spatial variations in the efficacy of any particular method of control. Provided insects do not move between sites, variations can be incorporated into spatially independent models by requiring different sets of parameter values for different locations.

Complications arise, however, when insects are free to move; fluxes of insects between different sites require models with explicit spatial terms to describe this movement. The example considered by Manoranjan and van den Driessche [19] (in the context of SIRM) and by Ludwig et al. [18] (in the context of spruce budworm populations) is that of environments favorable to insects interspersed with hostile regions. This scenario could arise from spraying an area with pesticide selectively, in a striplike pattern. Sprayed regions would be hostile, and the remaining areas favorable. Analytical and numerical results indicate that, in this case, persistence of the insect pest is conditional upon the size of the favorable environment exceeding a critical value. In other words, the strip spacing for spraying must be sufficiently small to ensure eradication of the pest. Other examples of this approach to spatial processes in ecology are given in [23].

In this paper we make a second argument for considering space in models for SIRM, even in the absence of any environmental variation. We show that the combined effects of dispersal terms and growth dynamics can amplify and modify small variations in the original distribution of fertile insects until a traveling wave of fertile insects forms, advancing (or retreating) across a region with a constant velocity, as an invasion (or an extinction). The wave arises from the combined effects of dispersal terms and growth dynamics; neither of the terms independently is sufficient to trigger a traveling wave. (See, e.g., [22] for a discussion of traveling waves.) We will show, for realistic parameter values, that models neglecting insect dispersal predict persistence of an outbreak while models including dispersal terms predict the antithesis —a wave of extinction. A strong argument for including space and movement in models for SIRM is thus provided.

It transpires that it is the density of sterile insects (or, alternatively, their release rate) that determines the velocity of the traveling wave. Provided the density (or release rate) of sterile pests is sufficiently low, the wave velocity is positive and the fertile insects invade, but when the density (or the release rate) of sterile insects exceeds a critical value, the wave velocity is negative and a retreating wave of extinction arises.

In this paper we briefly review the biological background and typical parameter values (Section 2) before listing the assumptions that go into our models (Section 3). We employ two approaches to the modeling and analysis: (i) detailed mathematical and numerical analyses for a simpler single-equation model (Section 4) and (ii) numerical simulations for a more complex two-equation model (Section 5). We then draw biological conclusions based upon the behavior of the two models and discuss strengths and weaknesses of the models and areas for further research (Section 6).

2. BIOLOGICAL BACKGROUND

Our goal is to use biologically realistic parameter values in determining the behavior of traveling waves resulting from the SIRM. While exact parameter values depend critically upon the particular pest and its ecosystem, order-of-magnitude estimates are possible.

We will show in succeeding sections, however, that analytical and numerical results regarding the system behaviors depend, not upon precise parameter values, but rather upon the magnitude of few critical parameter ratios. Although translations into precise estimates for densities and wave speeds eventually require exact data, we are able to make definite predictions about qualitative behaviors for a wide variety of insect pests.

Key life history parameters for the control of insect pests include the reproductive rate, survivorship, and carrying capacity. We now list typical ranges for parameter values. Values for the birth rate (a_1) are approximately 2–25 offspring per individual per day, with tse-tse flies at the low end of the scale and fruit flies at the high end. At low densities, survivorship S typically lies between 0.55 and 0.9 per day, thus predicting instantaneous density-independent death rates ($a_2 = -\ln S$) in the range $0.1 \leqslant a_2 \leqslant 0.6$. Biologically realistic values for the ratio of density-independent death to birth rates thus lie in the range $0 \leqslant A \leqslant 0.3$ ($A = a_2 / a_1$). Carrying capacities may be 10–10,000 per hectare, with typical values of 100–1000 hectare^{-1}.

Movement rates for insects, given in terms of mean squared displacement per day (m^2/day), vary greatly between different species but are often lower for sterile insects; the sterilization process can actually reduce mobility. In an experiment by Hamada [12] the dispersal of melon flies irradiated with 10,000 R was significantly reduced. For example, 33% of the control (nonirradiated) flies were captured at a station 50 m distant from the release site, but only 8% of the irradiated flies were captured there. Lower levels of irradiation (5000 and 7000 R) also reduced the dispersal ability of melon flies, but to a lesser extent.

3. MODELING ASSUMPTIONS

We base our description of birth and death dynamics upon the deterministic, continuous-time, density-dependent model of Barclay and Mackauer [4]. Other classes of models have been applied to the SIRM, including stochastic and discrete-time models, the relative merits of which are discussed in [7].

Barclay and Mackauer [4] gave explicitly the assumptions that went into their model, commenting that these would seem to apply to a wide range of biological situations. For the sake of completeness, the assumptions are reproduced here in a slightly modified form (see [2]):

(1) Populations exist as a continuum and reproduce continuously over time.

(2) Population growth follows a logistic curve.

(3) The carrying capacity of a given environment is constant.

(4) Sterile males are fully competitive with fertile males.

(5) Mating is at random, and the proportion of fertile matings is in direct proportion to the number of sterile and fertile individuals present in the population.

(6) Sterile sperm is fully competitive with fertile sperm.

(7) Each individual mates a random number of times; the number of matings follows a Poisson distribution with an identical mean for all individuals.

(8) The population sex ratio is 1-to-1 throughout life.

(9) The release of sterile individuals is continuous and at a constant rate per unit of time and per unit of habitat.

(10) The release of sterile individuals leads to the complete and instantaneous mixing of wild and treated individuals.

For analysis of our initial single-equation model (Section 4), we modify assumption (9) to the more restrictive assumption, which is that the release of sterile individuals is maintained so that there is a constant density of steriles. The unmodified assumption (9) is adopted for our more complex two-equation model (Section 5). Our extension of Barclay and Mackauer's [4] model lies in the important addition of dispersal terms for the fertile and sterile insects (see also [19]); insects are assumed to disperse randomly by means of simple one-dimensional diffusion (see, e.g., [23]). We then analyze our quantitative models for invasions and extinctions by means of traveling waves—a new phenomenon in the context of the SIRM—and draw conclusions regarding the impact that such waves may have on the biological outcome of SIRMs.

4. SINGLE-EQUATION MODEL

We initially assume that biocontrol treatment maintains the density of sterile insects ($2n$) at a constant level. The density of sterile females is thus n by assumption (8) in Section 3. Thus,

$$\frac{\partial u}{\partial t}=\left(\frac{a_1 u}{u+n}-a_2\right)u-2gu(u+n)+D\frac{\partial^2 u}{\partial x^2}, \tag{1}$$

where $u(x,t)$ denotes the density of fertile females ($\equiv$ density of fertile males, measured as number of insects per hectare), a_1 is the birth rate (measured as number of female offspring per day per individual female), a_2 is the density-independent death rate (per day), g is the density-dependent death rate [measured as hectares per insect per day and given by $2g=(a_1-a_2)/\text{carrying capacity}$], and D is the mean squared rate of spread (measured as square meters per day and assumed to be constant). To facilitate assessment of ecologically relevant parameters and to simplify analysis, we nondimensionalize (1), choosing

$$x^*=x\sqrt{\frac{a_1}{D}}, \qquad t^*=ta_1, \qquad u^*=u\frac{g}{a_1}, \qquad n^*=n\frac{g}{a_1}, \qquad A=\frac{a_2}{a_1}. \tag{2}$$

Dropping asterisks for notational simplicity, we rewrite (1) as

$$\frac{\partial u}{\partial t}=f(u;n)+\frac{\partial^2 u}{\partial x^2}, \tag{3}$$

where

$$f(u;n)=u\left(\frac{u}{u+n}-A-2(u+n)\right), \tag{4}$$

with the initial condition

$$u(x,0)=u^0(x). \tag{5}$$

The qualitative behavior of this model thus depends upon a single dimensionless parameter ($A=a_2/a_1$), the ratio of the density-independent death rate to the birth rate.

4.1. *INVASION OR EXTINCTION?*

In the absence of sterile individuals ($n = 0$), $f(u;0)$ is quadratic with roots at $u = 0$ and $u = (1 - A)/2$ [see Eq. (4)]. In such a case, Equation (3) reduces to the well-known logistic equation with diffusion, which is also known as Fisher's equation. A spatially uniform steady-state solution to (3), corresponding to the extinction of fertile insects is given by the trivial root of $f(u;0)$; another spatially uniform steady-state solution, corresponding to the outbreak of fertile insects, is given by the positive root of $f(u;0)$.

If the fertile insects are initially introduced into a local, bounded region, invasion can result when they reproduce and spread across the solution domain. This is evident from the well-known result that, provided initial conditions have compact support, the solution to Fisher's equation asymptotically approaches a traveling wave that sweeps across the domain with a fixed wave velocity [22], joining the extinction steady state ($u = 0$) to the invasion steady state [$u = (1 - A)/2$].

When sterile individuals are introduced ($n > 0$), the function defining birth and death dynamics for fertile insects [$f(u;n)$] undergoes an important qualitative change in shape, from a quadratic form to an essentially cubic form (Figure 1). In this latter case there are either one or three real roots for $f(u;n)$, depending upon whether n is greater than or less than the value $n_c = (1 - A)^2/8$ (Figure 1). Thus the roots for $f(u;n)$ are $u = 0$ and, when $0 < n < n_c$, $u = \hat{u}^-(n)$ and $u = \hat{u}^+(n)$, where

$$\hat{u}^{\pm}(n) = -n + \frac{(1-A) \pm \left[(1-A)^2 - 8n\right]^{1/2}}{4} > 0. \tag{6}$$

Locally stable, spatially uniform steady-state solutions to (3) are given by the smallest and largest roots of $f(u;n)$. The smallest root [$u(x,t) = 0$] corresponds to an extinction steady-state solution, and the largest root [$u(x,t) = \hat{u}^+(n)$] corresponds to an outbreak steady-state solution. Stability arises from the fact that $f'(0;n) < 0$ and $f'(\hat{u}^+(n);n) < 0$. The third root, $\hat{u}^-(n)$, corresponds to an unstable steady-state solution [$f'(\hat{u}^-(n);n) > 0$].

Our model predicts that, in the absence of sterile individuals a population of fertile insects will invade and spread into the new environment. However, by introducing sterile females (n) at a sufficiently high density in (3), (4), such an invasion can be effectively prevented or reversed. For example, if n exceeds n_c, then the outbreak steady state is eliminated, and the fertile population density (u) asymptotically approaches the extinction steady-state solution. However, we will show that, providing the initial condition (5) meets some very general criteria,

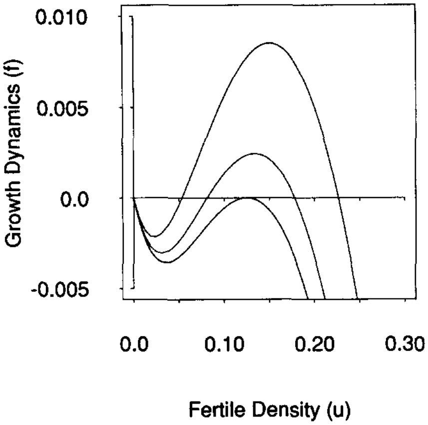

FIG. 1. Growth dynamics for $n > 0$ [Eq. (4)]. Curves are shown for $A = 0$ and $n = 0.1100$ (upper), $n = n_0 = 0.12029$, and $n = n_c = 0.1250$ (lower).

the population of fertile insects can go extinct even when the sterile females are present at levels that are substantially lower than the threshold n_c. This can occur by means of a traveling wave of extinction, joining the outbreak steady state to the extinction steady state and sweeping across the solution domain.

Our mathematical approach will be to determine a class of stable traveling wave solutions to (3), (4) parameterized by the density of steriles (n) and to determine constraints upon the initial conditions (5) that guarantee uniform convergence to the traveling wave solution. We implicitly assume that $0 < n < n_c$.

Traveling wave solutions to (3), (4) are expressed in terms of the moving coordinate $z = x - ct$, where $u(x,t) = U(z)$. Without loss of generality we consider solutions that join the outbreak steady state $[u = \hat{u}^+(n)$ as $z \to -\infty]$ to the extinction steady state ($u = 0$ as $z \to \infty$). When the wave velocity is positive ($c > 0$) the wave moves to the right and there is an invasion, and when the wave velocity is negative ($c < 0$) the wave moves to the left and there is an extinction.

Substituting the traveling wave form into (3) and applying boundary conditions described above, we observe that traveling wave solutions satisfy

$$cU' + f(U;n) + U'' = 0, \tag{7}$$

$$\lim_{z \to -\infty} U(z) = \hat{u}^+(n), \qquad \lim_{z \to \infty} U(z) = 0, \tag{8}$$

where a prime denotes differentiation with respect to z. This is an eigenvalue problem for the wave velocity $c(n)$.

Using results from [9], it can be shown that for $0 < n < n_c$ there exists a unique (modulo translation in z) solution to (7), (8) with a corresponding unique wave velocity c. A key feature in determining the existence and uniqueness of this traveling wave solution is the fact that $f'(0;n) < 0$ and $f'(\hat{u}^+;n) < 0$. Sufficient conditions on initial datum (5) for convergence to the traveling wave solution are

$$\lim_{x \to -\infty} \inf u^0(x) > \hat{u}^-(n), \qquad \lim_{x \to \infty} \sup u^0(x) < \hat{u}^-(n), \tag{9}$$

where $\hat{u}^-(n)$ is given by Equation (6) [9]. Thus the solution to (3)–(5) converges asymptotically to a traveling wave solution, satisfying (7), (8), providing that the initial condition (5) satisfies (9).

We now show that the direction of the traveling wave solution [sgn(c)] critically depends upon the value of n. Analysis of (7), (8) in the UU' phase plane indicates that the unique solution has a slope $U' < 0$ for $z \in (-\infty, \infty)$ and that $\lim_{z \to \pm\infty} U'(z) = 0$. Thus, multiplying (7) by U', integrating over the range $-\infty < z < \infty$, and applying the boundary conditions (8), we obtain

$$c\int_{-\infty}^{\infty} [U'(z)]^2 dz = F(\hat{u}^+(n);n), \tag{10}$$

where

$$F(u;n) = \int_0^u f(\mu;n)\, d\mu \tag{11}$$

and f is given by (4). The direction of the traveling wave solution [sgn(c)] is thus given by sgn[$F(\hat{u}^+(n);n)$].

We define n_0 as the value of n yielding a stationary ($c = 0$) solution to (7), (8). Accordingly n_0 is determined uniquely by

$$\begin{aligned} 0 &= F(\hat{u}^+(n_0);n_0) \\ &= -\frac{2}{3}[\hat{u}^+(n_0)]^3 + [1 - A - 2n_0]\frac{[\hat{u}^+(n_0)]^2}{2} \\ &\quad + n_0\left[-\hat{u}^+(n_0) + n_0 \ln\left(1 + \frac{\hat{u}^+(n_0)}{n_0}\right)\right] \end{aligned} \tag{12}$$

[see Eq. (10)].

We are not able to give exact analytical solutions to (7), (8), (4), but we are able to determine the qualitative behavior of a traveling wave solution near the point $n = n_0$. If the number of sterile insects drops below the critical value, then the integral of the growth dynamics increases [$F(\hat{u}^+(n);n) > 0$] (Figure 2), the wave velocity is positive [Eq. (10)], and initial conditions satisfying (9) result in an invasion. Conversely, if the number of sterile insects increases above the critical value, then the integral of the growth dynamics decreases [$F(\hat{u}^+(n);n) < 0$] (Figure 2), the wave velocity is negative [Eq. (10)], and initial conditions satisfying (9) result in an extinction.

The relationship between $n - n_0$ and $F(\hat{u}^+(n);n)$, shown graphically in Figure 2, can be determined to leading order by using the expansion

$$F(\hat{u}^+(n);n) = K(n_0)(n - n_0) + \mathcal{O}([n - n_0]^2), \tag{13}$$

where $K(n_0) < 0$ is given in Appendix A. This approximation, which is most accurate for n close to n_0 (Figure 2), suggests the utility of regular perturbation methods for calculating the traveling wave profile $U(z)$ and the wave velocity $c(n)$ for small $|n - n_0|$. In this paper we use such methods, as well as numerical solutions, in determining the shape and velocity of traveling wave solutions to (7), (8), (4).

4.2. *TRAVELING WAVE SOLUTIONS USING REGULAR PERTURBATION METHODS*

Defining $|n - n_0| = \varepsilon$, where n_0 satisfies (12) and $0 < \varepsilon \ll 1$, we have

$$n = n_0 + \nu\varepsilon, \qquad \nu = \pm 1. \tag{14}$$

We rewrite the function (4) as

$$f(u;n) = \phi(u;\varepsilon) = \sum_{j \geqslant 0} \varepsilon^j \phi_j(u) \tag{15}$$

and the integral (11) as

$$F(u;n) = \Phi(u;\varepsilon) = \int_0^u \phi(\mu;\varepsilon)\,d\mu = \sum_{j \geqslant 0} \varepsilon^j \Phi_j(u), \tag{16}$$

where

$$\Phi_j(u) = \int_0^u \phi_j(\mu)\,d\mu. \tag{17}$$

The larger root for $\phi(u, \varepsilon)$, given by (6), is rewritten and expanded as a

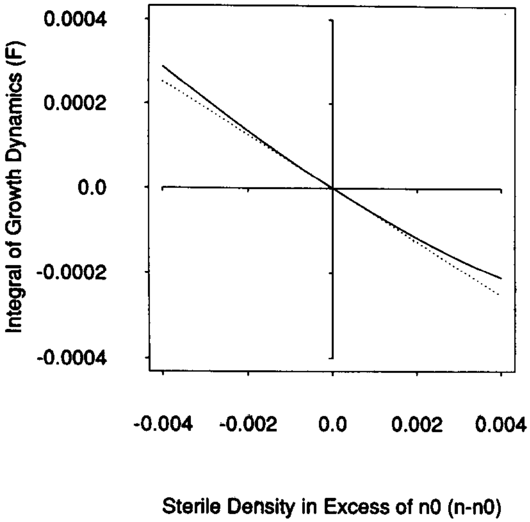

FIG. 2. Graphical representation of relationship between $n - n_0$ and $F(\hat{u}^+(n); n)$ shown here for $A = 0$ and n close to $n_0 = 0.12029$ (solid line). The dotted line shows $K(n_0)(n - n_0)$ [see Eq. (13)], where K is given in Appendix A.

regular series in ε:

$$\hat{u}^+(n) = \bar{u}^+(\varepsilon) = \sum_{j \geq 0} \varepsilon^j \bar{u}_j^+. \tag{18}$$

The first two terms of the series (15), (16), and (18) are given in Appendix B.

The traveling wave problem (7), (8) can thus be expressed as

$$cU' + \phi(U; \varepsilon) + U'' = 0, \tag{19}$$

$$\lim_{z \to -\infty} U(z) = \bar{u}^+(\varepsilon), \qquad \lim_{z \to \infty} U(z) = 0. \tag{20}$$

To calculate an approximate solution to this problem, we assume regular asymptotic expansions in terms of ε for the traveling wave solution and the wave velocity so that

$$U(z) = \sum_{j \geq 0} \varepsilon^j U_j(z), \tag{21}$$

$$c = \sum_{j \geq 0} \varepsilon^j c_j, \tag{22}$$

and substitute these expressions into (19), (20). The resulting $\mathscr{O}(1)$ problem is

$$c_0 U_0' + \phi_0(U_0) + U_0'' = 0, \tag{23}$$

$$\lim_{z \to -\infty} U_0(z) = \bar{u}_0^+, \qquad \lim_{z \to \infty} U_0(z) = 0, \tag{24}$$

and the $\mathscr{O}(\varepsilon)$ problem is

$$c_1 U_0' + c_0 U_1' + U_1 \frac{d\phi_0}{du}(U_0) + \phi_1(U_0) + U_1'' = 0, \tag{25}$$

$$\lim_{z \to -\infty} U_1(z) = \bar{u}_1^+, \qquad \lim_{z \to \infty} U_1(z) = 0. \tag{26}$$

The two systems (23), (24) and (25), (26) contain unknown quantities c_0 and c_1. As we now show, these unknown wave velocity coefficients can be derived using Equation (10).

Employing (11), (16), and (18), we observe that

$$\Phi_0(\bar{u}_0^+) = \Phi(\bar{u}^+(0);0) = F(\hat{u}^+(n_0);n_0) = 0. \tag{27}$$

Equations (15), (16), and (18) also yield

$$\frac{d\Phi_0}{du}(\bar{u}_0^+) = \phi_0(\bar{u}_0^+) = \phi(\bar{u}^+(0);0) = 0. \tag{28}$$

Using these results and Equation (16), we expand $\bar{u}^+(\varepsilon)$ about the point $\bar{u}_0^+$, rewriting Equation (10) as

$$\begin{aligned} c\int_{-\infty}^{\infty} & [U'(z)]^2\,dz \\ &= \Phi(\bar{u}^+(\varepsilon);\varepsilon) = \Phi_0(\bar{u}^+(\varepsilon)) + \varepsilon\Phi_1(\bar{u}^+(\varepsilon)) + \mathscr{O}(\varepsilon^2) \\ &= \Phi_0(\bar{u}_0^+) + \varepsilon\bar{u}_1^+\frac{d\Phi_0}{du}(\bar{u}_0^+) + \varepsilon\Phi_1(\bar{u}_0^+) + \mathscr{O}(\varepsilon^2) \\ &= \varepsilon\Phi_1(\bar{u}_0^+) + \mathscr{O}(\varepsilon^2). \end{aligned} \tag{29}$$

Substitution of the asymptotic expansions for $U(z)$ [Eq. (21)] and c [Eq. (22)] into Equation (29) yields

$$(c_0 + \varepsilon c_1)\int_{-\infty}^{\infty}\left\{[U_0'(z)]^2 + 2\varepsilon U_0'(z)U_1'(z)\right\}dz = \varepsilon\Phi_1(\bar{u}_0^+) + \mathscr{O}(\varepsilon^2).$$

Equating coefficients for successive powers of ε, we derive the $\mathscr{O}(1)$

equation,

$$c_0 \int_{-\infty}^{\infty} [U_0'(z)]^2 \, dz = 0, \tag{30}$$

and the $\mathscr{O}(\varepsilon)$ equation,

$$2c_0 \int_{-\infty}^{\infty} U_0'(z) u_1'(z) \, dz + c_1 \int_{-\infty}^{\infty} [U_0'(z)]^2 \, dz = \Phi_1(\bar{u}_0^+). \tag{31}$$

These two equations provide additional constraints to the systems (23)–(26), allowing us to determine the two unknown wave velocity coefficients, c_0 and c_1, when solving for the variables $U_0(z)$ and $U_1(z)$.

A solution, $U_0(z)$, to Equation (23) that is identically constant for all z cannot satisfy the boundary conditions (24). Thus Equation (30) gives $c_0 = 0$. This result is consistent with our choice of n_0 as the value of n yielding a stationary wave [see Eq. (12)]. Equations (23), (25), and (31) now simplify to yield

$$U_0'' = -\phi_0(U_0), \tag{32}$$

$$U_1 \frac{d\phi_0}{du}(U_0) + U_1'' = -c_1 U_0' - \phi_1(U_0), \tag{33}$$

$$c_1 \int_{-\infty}^{\infty} [U_0'(z)]^2 \, dz = \Phi_1(\bar{u}_0^+). \tag{34}$$

The boundary conditions for (32) and (33) are already given by (24) and (26).

Equation (34) can be simplified still further; multiplying Equation (32) by U_0' and integrating yields

$$(U_0')^2 = -2\Phi_0(U_0),$$

and thus (34) is rewritten as

$$c_1 = \frac{\Phi_1(\bar{u}_0^+)}{-2\int_{-\infty}^{\infty} \Phi_0(U_0(z)) \, dz} \tag{35}$$

or

$$c_1 = \frac{\Phi_1(\bar{u}_0^+)}{\int_0^{\bar{u}_0^+} [-2\Phi_0(\mu)]^{1/2} \, d\mu}. \tag{36}$$

Numerical quadrature of the denominator in Equation (36) [in conjunction with the definitions for n_0, $\Phi_0(\cdot)$, $\Phi_1(\cdot)$, and $\bar{u}_0^+$, which are (12), (60), (61), and (62), respectively], can be used to calculate c_1 directly in terms of the parameters A and ν [see Eqs. (4) and (14) for these parameters]. The traveling wave's velocity can thus be obtained to $\mathscr{O}(\varepsilon)$ without any knowledge of its shape.

4.3. *NUMERICAL SOLUTIONS*

As discussed in Section 4.1, $n = n_0$ yields a stationary wave solution for (3), (4) that links outbreak and extinction steady states. The solution is, in other words, a cline joining $u = \hat{u}^+(n_0)$ to $u = 0$. The value of n_0 given by Equation (12) depends upon the dimensionless parameter A. Results, shown in Figure 3, give the constant n_0 over the biologically relevant range of A $(0 \leqslant A \leqslant 0.3)$; see Section 2. Calculations used Newton's method to iteratively refine initial estimates for n_0. These values of n_0 lie below $n_c = (1 - A)^2/8$, the maximum possible value of n for which the outbreak steady state exists (Figure 3) (see also Section 4.1). Recall that in Section 4.1 we predicted the value of c in (7), (8) to be negative for $n_0 < n < n_c$ and to be positive for $0 \leqslant n < n_0$, the former case corresponding to an extinction wave and the latter to an invasion wave. In this section we provide quantitative estimates for c by evaluating the first-order wave velocity coefficient, c_1.

Before discussing the first-order wave velocity coefficient (Figure 3), we present numerical solutions for the stationary wave $(n = n_0)$. Because biologically relevant values for A are typically small (Section 2), we choose to calculate this stationary profile for the limiting case, $A \to 0$ $(n_0 = 0.12029)$. This solution is obtained on a finite domain $[-L, L]$ $(L = 14)$ by two different methods:

(1) Solution of the original nonlinear PDE system [(3)–(5)], with boundary conditions

$$u(-L,t) = \hat{u}^+(n_0), \qquad u(L,t) = 0,$$

and a step function initial condition that satisfies these boundary conditions. The method of lines and Gear's method were used to solve the PDE.

(2) Solution of the ODE equation describing the stationary traveling wave solution (32), with boundary conditions derived from (24) and given by

$$U_0(-L) = \bar{u}_0^+ = \hat{u}^+(n_0), \qquad U_0(L) = 0.$$

Newton's method was used to solve the ODE.

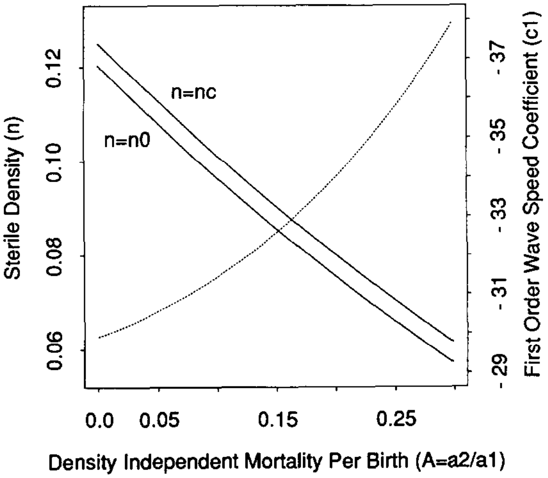

FIG. 3. Critical values for disappearance of the outbreak steady state (n_c) and for stationary wave solutions (n_0) are shown as a function of A over the biologically realistic range, $0 \leqslant A \leqslant 0.3$. The first-order wave speed coefficient (c_1) is also calculated for this range of A (dotted line).

The two solutions are shown in Figure 4. The solid line shows the ODE solution (method 2). Overlying this is the PDE solution (method 1), denoted by diamond-shaped symbols. Notice that the two solutions line up very closely with each other; any discrepancies between these solutions are only a result of approximation errors encountered in the numerical methods.

From our asymptotic analysis in Section 4.2, we know that values of n that are a distance ε away from n_0, Equation (14), can result in a non-zero traveling wave velocity given by Equation (22). We have already shown that the $\mathscr{O}(1)$ wave velocity term is $c_0 = 0$ (Section 4.2). Calculation of the $\mathscr{O}(\varepsilon)$ wave velocity term results from numerical integration of Equation (36) (Figure 3). For $A = 0$, the $\mathscr{O}(\varepsilon)$ correction to the wave velocity is

$$c_1 = -29.9\nu. \tag{37}$$

This constant (c_1) is also calculated using Equation (35) and numerical quadrature of the ODE solution (calculated by method 2, above, for $A = 0$ and shown in Figure 4). Limits of integration are ± 14 rather than $\pm\infty$ [as required by Eq. (35)], thereby introducing a source of truncation

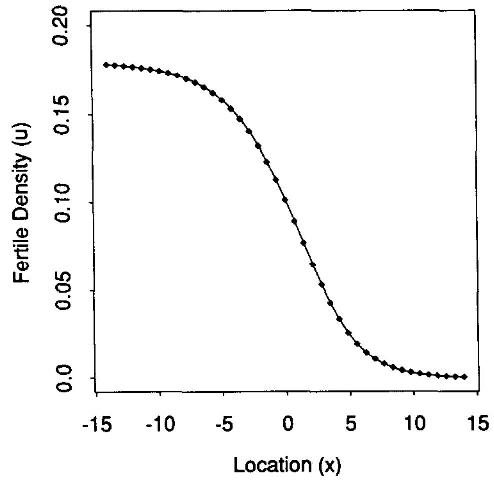

FIG. 4. The numerical solution for the ODE that describes a stationary traveling wave [Eq. (32)] is overlaid with the numerical solution for the analogous PDE [Eqs. (3)–(5) with $n = n_0$, i.e., $\varepsilon = 0$]. Boundary conditions are as described in Section 4.3. The ODE solution is represented by solid line and the PDE solution by diamonds.

error. The resulting value of c_1 is

$$c_1 = -30.1\nu, \tag{38}$$

which compares quite closely with that given by Equation (37).

Traveling wave solutions to the full PDE model [Eqs. (3)–(5)] are numerically simulated (see Figure 5). When $\varepsilon = 0.001$, average wave velocities of -0.0316 and 0.0284 result for $\nu = \pm 1$. As ε is decreased, the average wave velocity converges to approximately $-30\varepsilon\nu$, corresponding closely to the previous estimates given in (37) and (38) and indicating that for small ε an accurate estimate of the wave velocity is obtained when only the first two terms in the expansion for c are kept.

5. TWO-EQUATION MODEL

In this section we assume that the biocontrol treatment consists of *releasing* the sterile females $[n(x,t)]$ at a constant rate. Dynamics for both the sterile females and the fertile females $[u(x,t)]$ are now included. Thus

$$\frac{\partial u}{\partial t} = \left(\frac{a_1 u}{u+n} - a_2\right)u - 2gu(u+n) + D\frac{\partial^2 u}{\partial x^2}, \tag{39}$$

$$\frac{\partial n}{\partial t} = r - a_2 n - 2gn(u+n) + \tilde{D}\frac{\partial^2 n}{\partial x^2}, \tag{40}$$

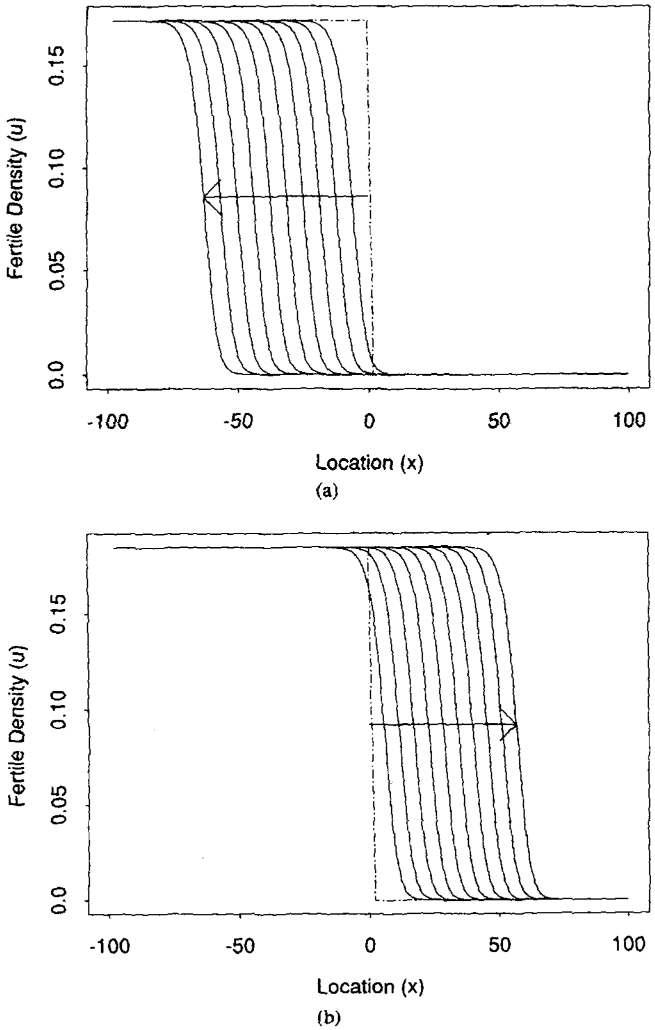

FIG. 5. Numerical solution to the full PDE model [Eqs. (3)–(5)] with zero-flux boundary conditions. The dashed line indicates initial conditions. Solutions are shown for time intervals of size 200. Parameter values are $A = 0$ and n defined by (14), with $n_0 = 0.12029$ and $\varepsilon = 0.001$. (a) The case $\nu = +1$ yields a wave with average velocity $c = -0.0316$; (b) the case $\nu = -1$ yields a wave with average velocity $c = 0.0284$.

where parameters are as described in Section 4, except that the additional parameters r and $\tilde{D}$ are the constant release rate for sterile insects (measured as number of sterile females released per hectare per day) and the diffusion coefficient for sterile insects (measured as square meters per day), respectively. Note that $\tilde{D}$ typically is less than D, as discussed in Section 2. To nondimensionalize we use (2) and

$$R = gr/a_1^2, \qquad \delta = \tilde{D}/D.$$

Equations (39) and (40) now become

$$\frac{\partial u}{\partial t} = f(u,n) + \frac{\partial^2 u}{\partial x^2}, \tag{41}$$

and

$$\frac{\partial n}{\partial t} = g(u,n) + \delta\frac{\partial^2 n}{\partial x^2}, \tag{42}$$

where

$$f(u,n) = u\left(\frac{u}{u+n} - A - 2(u+n)\right), \tag{43}$$

$$g(u,n) = R - An - 2n(u+n), \tag{44}$$

with initial conditions

$$u(x,0) = u^0(x), \qquad n(x,0) = n^0(x).$$

We briefly consider spatially homogeneous steady-state solutions to (41), (42). Results similar to those given below can also be found in [4] and [24]. The null cline for the spatially independent version of (41) is given by $f(u,n) = 0$ [see Eq. (43)]. Two nonzero roots for f [cf. Eq. (6)] satisfy

$$\frac{u}{u+n} - A - 2(u+n) = 0, \tag{45}$$

and the third root is zero (Figure 6). The null cline for the spatially independent version of (42), given by $g(u,n) = 0$ [see Eq. (44)], satisfies

$$u = -n + (R - An)/2n \tag{46}$$

(Figure 6).

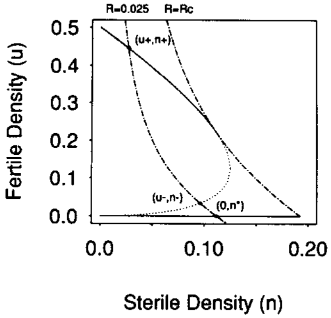

FIG. 6. The null cline for $f = 0$ ($A = 0$) is denoted by the upper solid line, the solid line at $u = 0$ (stable branches), and a dotted line (unstable branch). The null cline for $g = 0$ is denoted by a dashed line and is shown for $R = 0.025$ and $R = R_c = 0.0741$. [See Eqs. (43), (44) for details.] Steady-state solutions are shown for the case $R = 0.025$.

When $u = 0$, the steady-state value for n, given by (46), is

$$n^* = \left[-A + (A^2 + 8R)^{1/2} \right] / 4$$

(Figure 6). Substituting (46) into (45), we observe that when $u \neq 0$, steady-state values for n satisfy

$$h(n) = 2n^3 + An^2 - R(1 + A)n + R^2 = 0. \tag{47}$$

By Descartes' rule of signs, this equation is shown to have exactly one negative root and either two positive real roots (null clines intersect at $u > 0$) or two complex roots (null clines intersect only at $u = 0$). When the null clines intersect at $u > 0$ we denote the positive real roots to (47) by n^+ and $n^- > n^+$ and the corresponding values of u by $\hat{u}^+(n^+) = u^+$ and $\hat{u}^-(n^-) = u^-$ (Figure 6).

As the release rate for sterile insects (r) increases in relation to the birth rate for fertile insects (a_1) (R increasing), the $g = 0$ null cline moves to the right in Figure 6. A positive steady-state value for u requires that $R \leqslant R_c$, where R_c satisfies

$$h(n) = h'(n) = 0. \tag{48}$$

In other words, at $R = R_c$ the two positive roots for (47) (n^+ and n^-)

coalesce. Solving (48) we obtain a quadratic in R,

$$108R^2+4(1+A)\left[A-2(1-A)^2\right]R-A^2(1-A)^2=0 \qquad (49)$$

with positive root R_c.

5.1. *TRAVELING WAVES*

Linear analyses about the steady-state solutions for (41), (42) indicate that points (u^+,n^+) on the upper solid line in Figure 6 are locally stable to spatially homogeneous perturbations, as are points $(0,n^*)$ on the $u=0$ solid line. Points (u^-,n^-) on the intermediate dotted line in Figure 6 are, however, unstable to spatially homogeneous perturbations. The results arise directly from analysis of the community matrix, C, corresponding to the linearized version of (41), (42) (with spatial terms omitted) evaluated at a given steady state, namely

(1) If $u\neq 0$, then

$$\operatorname{tr} C=f_u+g_n=-[A+2(u+n)]^2-2(u+n)<0,$$

(2) If $u\neq 0$, then

$$\det C=f_u g_n-g_u f_n=-uh'(n)/[n(u+n)],$$

which is >0 if $(u,n)=(u^+,n^+)$ and is <0 if $(u,n)=(u^-,n^-)$, and
(3) If $u=0$, then the eigenvalues of C are $\{-(A+2n),-(A+4n)\}$.

For any fixed $R<R_c$ we thus have three steady-state solutions, with the outer two solutions $[(u^+,n^+)$ and $(0,n^*)]$ locally stable and the middle solution $(u^-,n^{)}$ unstable—a stability arrangement that qualitatively resembles that of the single-equation model (3), (4) in Section 4. It is natural to ask, therefore, whether traveling wave solutions also exist for this system, joining the outbreak steady state (u^+,n^+) to the extinction steady state $(0,n^*)$. Our approach is to conjecture the existence of such traveling wave solutions (in this section) and then to compute solutions numerically (in Section 5.2). It transpires that this two-equation system closely resembles the previous one-equation model in qualitative behavior, thereby suggesting that further in-depth mathematical analysis may yield little new biological insight. For example, to change (41), (42) to the previous one-equation model (3), (4), we would require n to be constant everywhere. But n varies little over traveling solutions such as the ones numerically computed in Section 5.2 and

shown in Figure 7 ($n^* - n^+$ is small), and so a simplification in which n remains constant is not unreasonable.

Traveling wave solutions to (41), (42), joining $(u,n)=(u^+,n^+)$ to $(u,n)=(0,n^*)$, satisfy

$$cU' + f(U,N) + U'' = 0, \tag{50}$$

$$cN' + g(U,N) + \delta N'' = 0, \tag{51}$$

$$\lim_{z \to -\infty} U = u^+, \qquad \lim_{z \to \infty} U = 0, \tag{52}$$

$$\lim_{z \to -\infty} N = n^+, \qquad \lim_{z \to \infty} N = n^*, \tag{53}$$

where U and N are functions of the moving coordinate, $z = x - ct$, so that $u(x,t) = U(z)$ and $n(x,t) = N(z)$.

For the single-equation model (3), (4) in Section 4, it was the fixed concentration of sterile insects (n) that determined the traveling wave velocity c. In our two-equation model, the concentration of steriles is no longer fixed but depends upon release and death rates. The release rate r can, however, be manipulated, thereby modifying the dynamics of the steriles through $R = gr/a_1^2$ [Eq. (44)].

Before discussing numerical solutions we determine how R affects the velocity of any traveling wave solution to (41), (42) [in other words, how R affects c in (50)–(53)]. In particular, we calculate the value of R (say, R_0) that yields a cline for (50)–(53) ($c = 0$). We use the fact that typical values for A are small (Section 2) and that $\delta \ll 1$ to determine R_0 analytically when A, $\delta \to 0$. For this case the value of N can be determined explicitly in terms of U:

$$N(U) = (1/2)\left[-U + (U^2 + 2R)^{1/2}\right] \tag{54}$$

because $g(U,N) = 0$ [see (44) and (51)]. The fact that $g(U,N) = 0$ also means that (43) simplifies to

$$f(U,N) = 2U[N(U/R - 1) - U]. \tag{55}$$

Using an approach analogous to that in Section 4.1, we multiply (50) by U' and integrate over $-\infty < z < \infty$ to obtain a necessary condition for the stationary solution:

$$\int_0^{u^+} 2U[N(U)(U/R - 1) - U]\,dU = 0, \tag{56}$$

where $N(U)$ is given in (54). The trigonometric substitution U

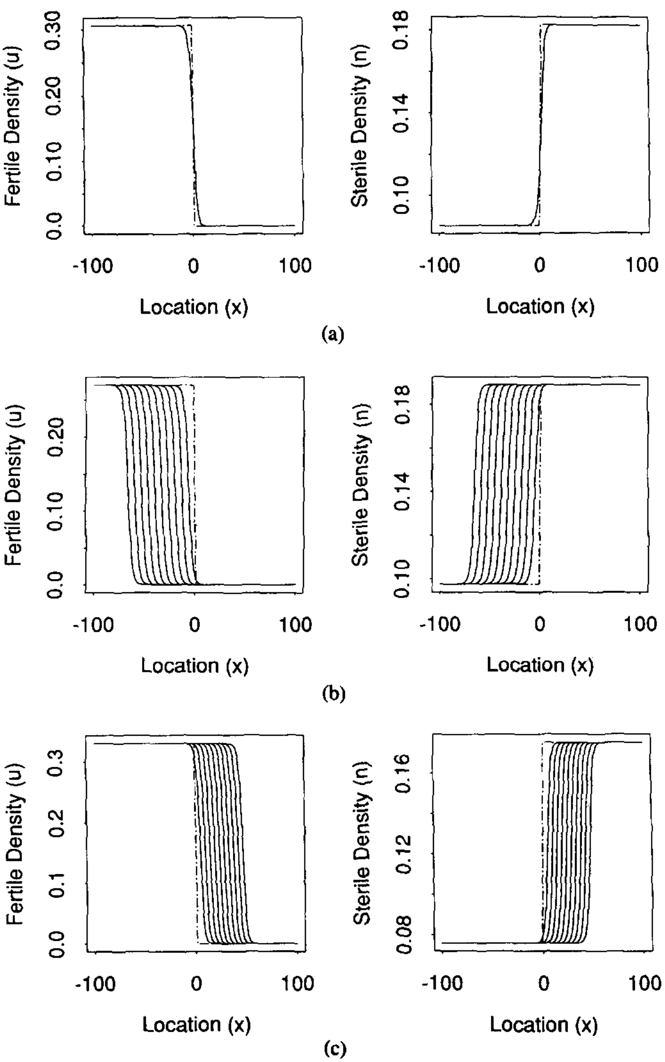

FIG. 7. Traveling wave solutions for the two-equation model (41)–(44), joining (u^+, n^+) to $(0, n^*)$ (see Figure 6), are given for $A = \delta = 0$. The dashed line indicates initial conditions. Solutions are shown for time intervals of size 50. (a) $R = R_0 = 0.06661$ yields a stationary wave solution; (b) $R = R_0 + 0.005$, a retreating wave of fertile extinction; and (c) $R = R_0 - 0.005$, an advancing wave of fertile invasion.

$=\sqrt{2R}\tan\theta$ can be used to integrate Equation (56) explicitly to yield

$$0=\left[-\frac{U^3}{3}-\frac{U^4}{4R}+\sqrt{U^2+2R}\left(-\frac{2R}{3}+\frac{U}{4}-\frac{U^2}{3}+\frac{U^3}{4R}\right)\right.$$
$$\left.-\frac{R}{2}\ln\left(U+\sqrt{U^2+2R}\right)\right]_0^{u^+}. \tag{57}$$

This equation must be satisfied by $R=R_0$, the release rate yielding a stationary solution. Note that the limit, u^+, in Equation (57) is also a function of R. [$u=u^+$ is given by (46) for $n=n^+$, the smaller positive root of (47) (see also Figure 6).]

5.2. *NUMERICAL SOLUTIONS*

Numerical solution of Equation (57), in conjunction with Equations (46) and (47), using Newton's method to iteratively refine an initial estimate for R, yields the root $R_0=0.06661$. A stationary wave results ($c=0$) in the absence of density-independent death ($A=0$) and in the absence of diffusion of sterile insects ($\delta=0$). The corresponding critical value for R, above which the outbreak steady state disappears, is calculated from (49) for the case $A=0$ as $R_c=0.07407$.

The existence of a traveling wave solution to the two-equation model (41), (42) was conjectured in Section 5.1, and it was predicted that $R=R_0$ would yield a stationary wave. Numerical solution of this PDE system with $A=0$ and $R=R_0$ does indeed result in a stationary wave profile (Figure 7a). Numerically calculated traveling wave solutions are shown for $R=R_0\pm0.005$ in Figures 7b and 7c. The former results in a traveling wave of extinction (Figure 7b), and the latter in a traveling wave of invasion (Figure 7c). The method of lines and Gear's method were used to solve the PDE system.

Relaxation of the assumption $\delta=0$ causes little change in R_0. For example, when $\delta=1$, numerical trial and error, solving the PDE system for various values of R, gives the new value of R_0 as 0.06555 (rather than $R_0=0.06661$).

6. DISCUSSION

The purpose of this paper is to show quantitatively how dispersal of insects, coupled with nonlinear growth terms, can result in waves of invasion or extinction. Even though this is the first time traveling wave solutions have been proposed for an SIRM model (as far as we are aware), the existence of wave solutions to this SIRM model is not surprising from a mathematical perspective; other bistable reaction–diffusion systems have been widely studied and analyzed, and general properties regarding traveling waves are well understood (see, e.g., [9]). (See also [17] for applications of such systems to dispersing asocial populations.) With a regular perturbation approach, we have, however, been able to quantitatively evaluate the effect of sterile individuals, and their release rate, upon the wave velocity and to calculate the wave profile to $\mathscr{O}(1)$.

Conditions on initial data for convergence to the traveling wave solution [see, e.g., (9)] strongly recommended the utility of controlling outbreaks by a joint strategy that combines SIRM with the spraying of a few selected areas. This would be sufficient to guarantee initiation of a traveling wave solution. Under these conditions our predictions for the asymptotic behavior of an SIRM system with dispersal differ dramatically from predictions where dispersal is not included in the SIRM model. In particular, when $n_0 < n < n_c$ (in the one-equation model, Section 4) or when $R_0 < R < R_c$ (in the two-equation model, Section 5), we predict a traveling wave of extinction while analysis of the analogous ODE model with no dispersal predicts persistence of an outbreak (see, e.g., [4]).

By necessity the mathematical models presented in this paper do not include all factors affecting sterile releases; some biological detail is sacrificed to make the models mathematically tractable. It is also hoped that by retaining only important biological details (which are fundamental to SIRMs) we achieve general results that are, at least to some extent, applicable to a wide variety of different release scenarios. The price we pay for these simplifications is in the predictive capacity of our models when applied to a specific release—precise predictions are far more likely to come from carefully tailored numerical simulations. Our discussion would therefore not be complete without mentioning possible violations of the model assumptions that were made in Section 3:

(1) The assumption that the carrying capacity of a given environment is constant (assumption 3 of Section 3); the carrying capacity, and thus the density-dependent death rate g, may vary between good and poor patches.

(2) The assumption that the release of sterile individuals is continuous and at a constant rate per unit time and per unit of habitat (assumption 9 of Section 3); it is unlikely that the release rate for sterile insects is uniform at all locations.

(3) The assumption of simple constant dispersal rates; this may inadequately reflect the true biology, as dispersal is likely to be lower in

a good patch (where food is abundant) than in a poor patch (where the insect pest may actively move around, looking for food).

(4) The assumption of dispersal in one spatial dimension; a more realistic model would include dispersal in two spatial dimensions rather than one.

Spatial variations in g and r (points 1 and 2 above) may mean that n (r) achieves a value above n_c (r_c) in some regions, but below n_c (r_c) in others. The regions in which critical parameter values are exceeded will quickly experience extinctions because the outbreak steady-state solution will have disappeared. Provided $n > n_0$ ($r > r_0$) everywhere, the remaining regions may then experience a more gradual extinction process by means of a traveling wave. In the case where $n < n_0$ ($r < r_0$) in some regions, a spatially heterogeneous stable steady-state solution may exist and the eradication program will have been only partly successful. Conceptually this is somewhat analogous to the spatial patterning problem discussed by Ludwig et al. [18] and Manoranjan and van den Driessche [19] (see also Section 1). Based on the above discussion, we postulate therefore that when g and r vary spatially, a sufficient condition for eradication of the insect pest is that $n > n_0$ ($r > r_0$) everywhere and that $n > n_c$ on a region large enough to initiate a traveling wave solution.

We expect that spatial variations in the diffusion rate (point 3 above) will result in corresponding variations of the wave velocity. Shigesada et al. [29] showed that this is the case for a traveling wave solution for Fisher's equation ($n = 0$) in variable environments.

The last point regarding dispersal in two spatial dimensions has, to some extent, been addressed analytically and numerically by Lewis and Kareiva [17] for asocial populations (i.e., $n > 0$ or $r > 0$). Results indicate that the two-dimensional analog of a traveling wave solution is a moving wave boundary, joining outbreak and extinction steady states. When the wave boundary is planar, the two-dimensional problem is reduced to one dimension by symmetry. Nonplanar waves propagate according to the curvature of an interface that marks the location of the wave front in $\mathbb{R}^2$. (See [17] for further details.) This problem is representative of a far larger class of interfacial problems in reaction–diffusion theory (see, e.g., [10]).

Further mathematical work, deriving analytical results for variable environments (points 1–3, above) or for dispersal in two spatial dimensions (point 4) would clearly be very useful. Alternatively, two-dimensional numerical simulations for (39), (40) could easily incorporate variable coefficients and could be tailored to fit particular release scenarios.

We are grateful to Dr. H. J. Barclay, Pacific Forestry Centre, Victoria, B.C., Canada for advice regarding typical parameter values and for valuable discussions. M.A.L. would like to thank NSERC of Canada for postdoctoral support. M.A.L. was also partially supported by a grant from the National Science Foundation (DMS-9222533). P.vdD. was partially supported by NSERC A-8965 and the University of Victoria Committee on Faculty Research and Travel.

APPENDIX A. EVALUATION OF $K(n_0)$

A series expansion of $F(\hat{u}^+(n), n)$ in terms of $(n - n_0)$ yields Equation (13), where

$$\begin{aligned}
K(n_0) &= \left[\frac{\partial}{\partial n} F(\hat{u}^+(n); n)\right]_{n=n_0} \\
&= f(\hat{u}^+(n_0); n_0)\left[\frac{\partial}{\partial n}\hat{u}^+(n)\right]_{n=n_0} \\
&\quad + \int_0^{\hat{u}^+(n_0)} \left[\frac{\partial}{\partial n} f(\mu; n)\right]_{n=n_0} d\mu \\
&= -\int_0^{\hat{u}^+(n_0)} \mu\left[\frac{\mu}{(\mu+n_0)^2} + 2\right] d\mu < 0 \\
&= -\left[\hat{u}^+(n_0) + n_0 - 2n_0 \ln\left(1 + \frac{\hat{u}^+(n_0)}{n_0}\right)\right. \\
&\qquad \left. - \frac{n_0^2}{\hat{u}^+(n_0) + n_0} + [\hat{u}^+(n_0)]^2\right].
\end{aligned}$$

APPENDIX B. TERMS IN EXPANSIONS FOR $\phi(u; \varepsilon)$, $\Phi(u, \varepsilon)$, AND $\bar{u}^+(\varepsilon)$

Using (4) and (14), the first two terms in series (15) are calculated to be

$$\phi_0(u) = u\left(\frac{u}{u+n_0} - A - 2(u+n_0)\right) \tag{58}$$

and

$$\phi_1(u) = -\nu u\left(\frac{u}{(u+n_0)^2} + 2\right), \tag{59}$$

whose integrals, defined by (17), are

$$\Phi_0(u) = -\frac{2}{3}u^3 + (1 - A - 2n_0)\frac{u^2}{2} + n_0\left[-u + n_0 \ln\left(1 + \frac{u}{n_0}\right)\right], \quad (60)$$

$$\Phi_1(u) = -\nu\left[u + n_0 - 2n_0 \ln\left(1 + \frac{u}{n_0}\right) - \frac{n_0^2}{u + n_0} + u^2\right]. \quad (61)$$

Using (6) and (14), the first two terms in series (18) are calculated to be

$$\bar{u}_0^+ = -n_0 + \frac{(1-A) + \left\{(1-A)^2 - 8n_0\right\}^{1/2}}{4}, \quad (62)$$

and

$$\bar{u}_1^+ = -\nu\left(1 + \frac{1}{\left\{(1-A)^2 - 8n_0\right\}^{1/2}}\right). \quad (63)$$

REFERENCES

1 H. J. Barclay, The sterile release method for population control with interspecific competition, *Res. Popul. Ecol.* 23:145–155 (1981).

2 H. J. Barclay, Demographic consequences of monogamy and polygamy for a sterile release program, *Protect. Ecol.* 6:209–217 (1984).

3 H. J. Barclay, Models for pest control: complementary effects of periodic releases of sterile pests and parasitoids, *Theor. Pop. Biol.* 32:76–89 (1987).

4 H. Barclay and M. Mackauer, The sterile insect release method for pest control: a density-dependent model, *Environ. Entomol.* 9:810–817 (1980).

5 A. H. Baumhover, A. J. Graham, B. A. Bitter, D. E. Hopkins, W. D. New, F. H. Dudley, and R. C. Bushland, Screwworm control through release of sterilized flies, *J. Econ. Entomol.* 48:462–466 (1955).

6 A. A. Berryman, Mathematical description of the sterile male principle, *Can. Entomol.* 99:858–865 (1967).

7 W. G. Costello and H. M. Taylor, Mathematical models of the sterile male technique of insect control, in *Mathematical Analysis of Decision Problems in Ecology* (Lect. Notes Biomath., 5), A. Charnes and W. R. Lynn, Eds., Springer-Verlag, Berlin, 1975, pp. 318–359.

8 K. Dietz, The effect of immigration on genetic control, *Theor. Popul. Biol.* 9:58–67 (1976).

9 P. Fife, *Mathematical Aspects of Reacting and Diffusing Systems* (Lect. Notes Biomath. 28), Springer-Verlag, Berlin, 1979.

10 P. Fife, *Dynamics of Internal Layers and Diffusive Interfaces* (CBM –NSF Regional Conf. Ser. Appl. Math.), SIAM, Philadelphia, 1988.

11 H. M. Graham, Sterile pink bollworm: field releases for population suppression, *J. Econ. Entomol.* 71:233–235 (1978).

12 R. Hamada, Studies on the dispersal behavior of melon flies, *Dacus curcurbitae* Coquillett (Diptera: Tephritidae), and the influence of gamma-irradiation on dispersal, *Appl. Entomol. Zool.* 15:363–371 (1980).

13 G. W. Harrison, H. J. Barclay, and P. van den Driessche, Analysis of a sterile release model with predation, *J. Math. Biol.* 16:33–48 (1982).

14 O. Iwahashi, Eradication of the melon fly, *Dacus curcurbitae*, from Kume Is., Okinawa, with the sterile insect release method, *Res. Popul. Ecol.* 19:87–98 (1977).

15 E. F. Knipling, Possibilities of insect control or eradication through the use of sexually sterile males, *J. Econ. Entomol.* 48:459–462 (1955).

16 E. S. Krafsur, H. Townson, G. Davidson, and C. F. Curtis, Screwworm eradication is what it seems, *Nature* 323:495–496 (1986).

17 M. A. Lewis, and P. Kareiva, Allee dynamics and the spread of invading organisms, *Theor. Popul. Biol.* 43, (in press).

18 D. Ludwig, D. G. Aronson, and J. F. Weinberger, Spatial patterning of the spruce budworm, *J. Math. Biol.* 8:217–258 (1979).

19 V. S. Manoranjan and P. van den Driessche, On a diffusion model for sterile insect release, *Math. Biosci.* 79:199–208 (1986).

20 F. Mautner Markhof, Ed., *Computer Models and Applications of the Sterile Male Technique*, Panel Proceedings, IAEA, Vienna, 1973.

21 D. R. Miller and D. E. Weidhaas, Equilibrium populations during a sterile release program, *Environ. Entomol.* 3:211–216 (1974).

22 J. D. Murray, *Mathematical Biology*, Springer-Verlag, Berlin, 1989.

23 A. Okubo, *Diffusion and Ecological Problems: Mathematical Models*, Springer-Verlag, New York, 1980.

24 S. Parkinson, Thesis for MSc. in mathematics, Oxford Univ., Oxford, U.K., 1985.

25 R. E. Plant and R. T. Cunningham, Analyses of the dispersal of sterile Mediterranean fruit flies (Diptera: Tephritidae) released from a point source, *Environ. Entomol.* 20:1493–1503 (1991).

26 R. E. Plant and M. Mangel, Modeling and simulation in agricultural pest management, *SIAM Rev.* 29:235–261 (1987).

27 T. Prout, The joint effects of the release of sterile males and immigration of fertilized females on a density regulated population, *Theor. Popul. Biol.* 13:40–71 (1978).

28 M. D. Proverbs, J. R. Newton, and D. M. Logan, Codling moth control by the sterility method in twenty-one British Columbia orchards, *J. Econ. Entomol.* 70:667–671 (1977).

29 N. Shigesada, K. Kawasaki, and E. Teramoto, Travelling periodic waves in heterogeneous environments, *Theor. Popul. Biol.* 30:143–160 (1986).